ELSEVIER

Surface Science 336 (1995) 280–286

surface science

Adsorption of carbon dioxide by ferroelectric lithium niobate

A.L. Cabrera [a,*], F. Vargas [a], J.J. Albers [b]

[a] *Pontificia Universidad Catolica de Chile, Facultad de Fisica, Casilla 306, Santiago 22, Chile*

[b] *Universität des Saarlandes, Fachrichtung 10.3, Technische Physik, Postfach 1150, Bau 38, 3.OG, D-66041 Saarbrücken, Germany*

Received 13 January 1995; accepted for publication 28 March 1995

Abstract

Desorption curves of CO_2 are presented for powder of lithium niobate with main particle sizes of 1000, 500, 200, 100 and 50 μm in diameter. The percentage of surface area occupied by CO_2 molecules is calculated after measuring the total surface area of the samples using N_2 single point BET. Adsorption of CO_2 and N_2 were measured with a Quantasorb instrument using flowing helium. The ratio of the surface area covered by CO_2 with respect to N_2 changes from 11.5% for the 50 μm particles down to 6.7% for the 100 μm particles. Adsorption of CO_2 for particles equal to or larger than 200 μm could not be measured with our technique. XPS results on a single piece of lithium niobate indicated that CO_2 is adsorbed on the surface when only Nb^{3+} ions are present. Induced crystallographic transformation of the crystal by an applied 2.5 kV field changes its surface composition from an initial mixture of Nb^{5+} and Nb^{3+} ions to pure Nb^{5+} ions and as a consequence of this change, adsorbed CO_2 was released. A tentative explanation of these results is that the adsorption of the CO_2 molecules by the ferroelectric substrate is due to a particular local electrostatic potential created by surface ions, in agreement with Pacchioni's work on other oxide surfaces.

Keywords: Carbon dioxide; Chemisorption; Dielectric phenomena; Niobium; Photoemission; Polycrystalline surfaces; Solid–gas interfaces; Thermal desorption; Thermal desorption spectroscopy; X-ray photoelectron spectroscopy

1. Introduction

Our research interest is the search for anomalies observed in the rate of a surface reaction at the transition temperature of the substrate which heterogeneously catalyzed such a reaction. This type of effects are called Hedvall effects. The Hedvall effect of type I is associated with an abrupt increase or decrease in the reaction rate around the transition temperature but without a change in the activation energy, while the Hedvall effect of type II is associated with a change in activation energy when the substrate undergoes the phase transition. A change in the reaction rates above and below the phase transition might be related to the surface ability to adsorb the reactants in the different phases. We reported such an effect in the adsorption of CO_2 onto barium titanate in previous work [1].

Many examples of these effects were discussed in a paper by Voorhoeve [2] and a theoretical explanation intended by Suhl [3]. In the case of substrates which are ferroelectric materials, a similar effect can be expected since there are two phases present, ferroelectric and paraelectric. The phase transition in these materials is normally produced by a change in crystallographic structure. There are also few reports of anomalies found in reaction rates measured over ferroelectric crystals [4,5].

* Corresponding author. Fax: +56 2 5525916; E-mail: acabrera@lascar.puc.cl.

SSDI 0039-6028(95)00533-1

One possible explanation is that the dipole moment of a polar molecule (or induced dipole moment, as it is the case of CO_2 adsorbed over barium titanate [5]) interacts with the electric polarization of some ferroelectric domains at the surface. This interaction would then increase the strength of the molecular adsorption at the substrate's surface. We have pursued studies in the past to demonstrate this [1,6,7].

Another explanation is related to the ability of the surface oxide to adsorb the CO_2 molecule according to its basicity. Pacchioni discussed his work [8,9] on the adsorption of CO_2 on MgO and CaO, based largely on this explanation. For a ferroelectric crystal the electric transition occurs because it undergoes a crystallographic transition. A change in surface structure due to the transition should be reflected in a change of surface basicity as a result of a different configuration of surface ions.

We have studied reactions involving carbon monoxide (CO) and nitric oxide (NO) – both dipolar molecules – over potassium niobate ($KNbO_3$). We did not find an anomaly in the rates around the transition temperature (T_c) of potassium niobate (708 K). Since the surface area of the ferroelectric crystal was low, we were forced to measure the reaction rates over fine powder of the material in order to increase the amount of the products. Nevertheless, we noticed that the spontaneous polarization of the powder (in the range 30–60 μm in diameter), present in the ferroelectric state, was significantly depressed. This deterioration of the spontaneous polarization in ferroelectric crystals as a function of particle size is well documented [10].

More recently, we have studied adsorption of CO_2 by barium titanate crystals [1] with main particle sizes of 1000, 500, 200, 100 and 50 μm in diameter. The percentage of surface area occupied by CO_2 molecules is calculated after measuring the total surface area of the samples using N_2 single point BET [11]. The ratio of surface area covered by CO_2 with respect to N_2 changes from 50% for particle sizes between 1000 and 200 μm down to 19% for 50 μm particles. Spontaneous polarization measurements for samples with main particle sizes of 50 and 100 μm were made and they show a weak ferroelectric behavior, indicating that ferroelectricity is destroyed for these small particles. A tentative explanation of these results was the assumption that the adsorption of some CO_2 molecules on the ferroelectric substrate is mediated by a dipole–dipole coupling between the CO_2 molecules and the substrate.

Tamaru and co-workers [5] also claimed that the reason for the anomaly observed in the production of CO_2 from the oxidation of CO over barium titanate was the difference in CO_2 adsorption strength above and below the transition temperature of barium titanate (393 K). Tamaru and co-workers determined that the CO_2 molecule is adsorbed with the carbon near the surface and the oxygens standing up, away from the surface. This bend between the C–O bonds induces a dipole moment between the C and O atoms since the CO_2 molecule does not have any longer a linear shape.

From all this previous work, we should be able to ascertain whether or not the adsorption of CO_2 by ferroelectric oxides is mediated by a dipole–dipole interaction since the ferroelectricity is depressed when the crystal is reduced to small particles. We decided then to study the amount of CO_2 chemisorbed by lithium niobate powder with different main particle sizes to see if we could find a correlation in adsorption for all ferroelectric materials.

This work presents desorption curves of CO_2 for powder of lithium niobate with main particle sizes of 1000, 500, 200, 100 and 50 μm in diameter. The percentage of surface area occupied by CO_2 molecules is calculated after measuring the total surface area of the samples using N_2 single point BET [11]. Adsorption of CO_2 by a large crystal of lithium niobate was also studied with XPS in ultra-high vacuum conditions. The results are discussed in the light of Pacchioni's work.

2. Experimental

2.1. Gas adsorption measurements

Adsorption of CO_2 and N_2 BET areas of lithium niobate were measured with a Quantasorb instrument from Quantachrome Corporation, Syosset, New York.

The surface area of the lithium niobate powder was determined from N_2 adsorption according to the BET theory (11). BET theory explains that breaks in the adsorption isotherms of gases at temperatures

near their condensation points are due to the formation of multimolecular adsorbed layers. The Quantasorb instrument is capable of measuring the N_2 adsorption by a solid at different N_2 partial pressures. Single point BET refers to the use of only one N_2 partial pressure.

The BET surface areas for the lithium niobate powder were measured with this instrument without modifying it. A flowing mixture of 20% N_2 in He was passed through a glass cell containing the sample powder. The glass cell was then immersed in a liquid N_2 bath kept always at the same level. At liquid N_2 temperature, He will not adsorb while N_2 will physically adsorb on the sample surface. Adsorption and desorption of N_2 occurs when the sample is immersed into and then withdrawn from the liquid N_2 bath. Nitrogen concentration changes in the flowing mixture are sensed by a specially designed thermal conductivity detector.

The instantaneous signal height is proportional to the rate of adsorption or desorption and the total integrated area under the curve is proportional to the quantity of gas (N_2) adsorbed. The area is automatically digitally integrated by the instrument but we also connected the analog output of the Quantasorb to a data acquisition system interfaced with a 386-AT computer.

Typically, the signal was monitored for 350 s (or 600 s for CO_2 adsorption), with a sampling rate of a point every 2 s. The real time voltage signal was recorded using LabTech Notebook software (Laboratory Technologies Corporation, Wilmington, Massachusetts) and 6B modules from Analog Devices (Norwood, MA). This combination allows acquisition of voltage or current signals with variable sampling rates. The data were transferred to the computer for further analysis and plotting using an appropriate software.

A modification to the Quantasorb instrument was made to measure desorption of CO_2 from the lithium niobate. Because CO_2 is chemisorbed by the sample, desorption must be induced by heating the sample well above room temperature. A special glass cell was built which allowed the powder sample to be introduced in an electrical tube furnace. The sample was heated up to 700 K during desorption, and the temperature of the sample was monitored by a chromel–alumel thermocouple which was in close contact with the sample but was outside the glass cell. The powder sample inside the glass cell was outgassed in pure N_2 at 383 K for at least 1 h. Then, after the sample has cooled down to room temperature, the flowing gas was switched to pure CO_2 and kept under CO_2 for 15 min. After that, the gas flow was switched again to pure He and the sample was heated with a nearly linear rate (20 K/min) to 700 K. The CO_2 desorbed was registered as a peak with a maximum around 600 K. More details of this procedure can be found elsewhere (12).

The same glass sample cell was used to measure first the N_2 BET surface area and then the CO_2 chemisorption without removing the lithium niobate powder sample from it.

Calibrations of the integrated area under the curves were performed by injecting 1 ml of pure N_2 or CO_2 into the carrier stream. By doing that, the respective areas under the curves were correlated with an accurate amount of volume corresponding to the adsorbed gas.

Lithium niobate, 99.99% pure, was obtained from Cerac, Inc. (Milwaukee). Another piece of lithium niobate with a size of $1 \times 2 \times 5$ cm was grown at the University of Saarland and it was mainly used for N_2 and CO_2 adsorption measurements.

Powder samples with different grain sizes were obtained by crushing millimeter size crystals and sieving the material through sieves of different mesh sizes. 3 g samples of lithium niobate trapped between meshes with Tyler sizes 14–20, 20–50, 50–100, 100–200 and 200–325 were obtained. The average particle size of these samples corresponds to 1015, 551, 223, 111 and 59 μm respectively, but for the sake of simplicity we will refer to them as 1000, 500, 200, 100 and 50 μm throughout this paper.

High purity He and N_2 (99.999% pure) and 99.9% pure CO_2 from Matheson (AGA Chile) were used in all the experiments.

2.2. XPS studies

X-ray photoelectron spectroscopy (XPS) analyses were performed with a cylindrical mirror analyzer (CMA) from Physical Electronics. The analyzer was operated in the retarding mode using Mg Kα radiation (1253.6 eV). Survey spectra were scanned from 0 to 900 eV of binding energy with 100 eV of pass

energy (1.2 eV resolution). The binding energies for Nb, C and O were obtained from high-resolution scans using 50 eV of pass energy (0.6 eV resolution). More details of this system can be found elsewhere [13].

A single piece of lithium niobate crystal with dimensions of $0.8 \times 0.8 \times 0.2$ cm, with an almost flat surface, was used for the XPS characterization and CO_2 adsorption studies in UHV. The crystal was supported on a flat piece of quartz and four electrical contacts made of 302 ss were provided at the edges of the crystal. Each pair of contacts was positioned at opposite edges. During the experiments high voltage was applied to each pair of these contacts at different times as discussed in Section 3.

3. Results and discussion

Typical nitrogen adsorption curves for powders with particle sizes of 1000, 500, 100 and 50 μm are displayed in Fig. 1. Similar nitrogen desorption curves for the powder samples with different particle sizes were obtained. The amount of N_2 adsorbed at liquid N_2 temperature is proportional to the area under each curve. Moreover, this amount of N_2 adsorbed is proportional to the total surface area of the powder sample, assuming that a molecule of N_2 occupies a given surface area. We have assumed, after Emmett and Brunauer [14], that a N_2 molecule occupies 16.2×10^{-20} m^2. The curves in Fig. 1 indicate that the total surface area of the powder

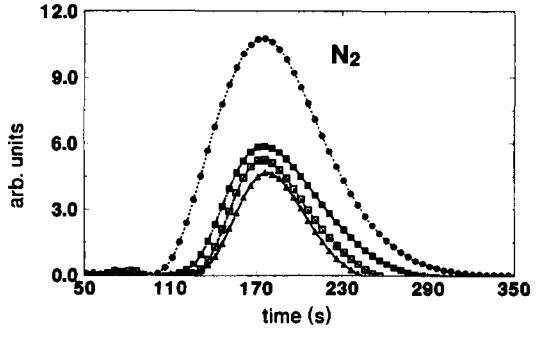

Fig. 1. Nitrogen BET adsorption curves for powder of lithium niobate with different particle sizes: (●) 50 μm; (■) 100 μm; (□) 200 μm; (▲) 1000 μm.

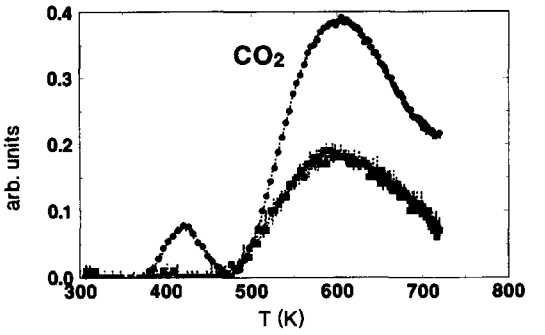

Fig. 2. Carbon dioxide desorption curves for powder of lithium niobate with different particle sizes: (●) 50 μm; (■) 100 μm.

samples monotonically increases as the particle size decreases, as was expected.

The corresponding CO_2 desorption curves for the same samples with particle sizes of 1000, 500, 100 and 50 μm were measured. Desorption of CO_2 was observed for the samples with particle sizes of 100 and 50 μm only and they are displayed in Fig. 2. The amount of CO_2 desorbed also decreases when the particle size increases. In this case, it decreases more rapidly than in the case of N_2 since CO_2 is not detectable for the 200 μm size sample. The signal is now noisier because when we heat the sample we also heat the flowing gas, upsetting the background signal.

The CO_2 desorption rate at each temperature can be calculated from the curves shown in Fig. 2 using the standard rate equation for desorption [13]. Plotting the logarithm of the rate as a function of the inverse absolute temperature (Arrhenius plot), the desorption energy was obtained and corresponds to -15.9 ± 0.5 kcal/mol. The Arrhenius plots for both curves shown in Fig. 2 are displayed in Fig. 3. This desorption energy which corresponds to about -0.7 eV is similar to the values obtained for CO_2 desorption from a MgO surface and lower than the value for desorption from CaO [9].

The amount of N_2 and CO_2 adsorbed by the samples with different particle sizes is listed in Table 1. The ratio of surface area covered by CO_2 and N_2 is also listed in the same table. One can clearly see that the ratio of area covered by CO_2 is between 6.7% and 11.5% for particle sizes between 100 and 50 μm. This is much smaller than in the case of CO_2

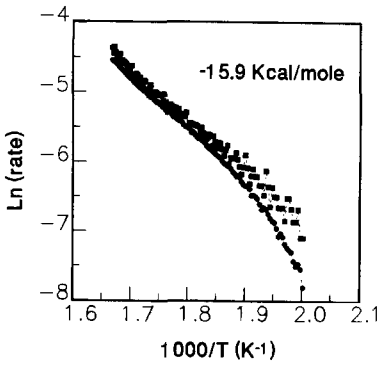

Fig. 3. Arrhenius plots of CO_2 desorption rate versus inverse absolute temperature for the desorption curves shown in Fig. 2. Full circles correspond to desorption from 50 μm powder and full squares correspond to desorption from the 100 μm powder.

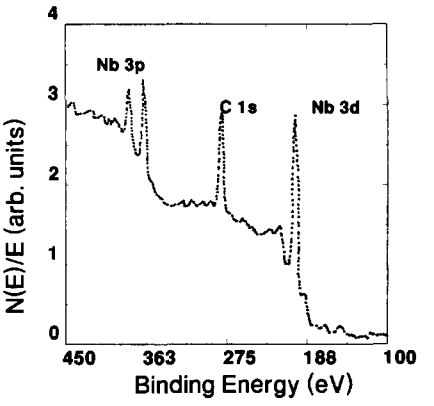

Fig. 4. XPS survey scan of a single piece of lithium niobate.

adsorption by barium titanate (between 19% and 50%).

A small piece of the lithium niobate crystal was placed inside a vacuum chamber provided with surface analysis facilities (AES, XPS, mass spectrometer and Ar sputtering gun). After the vacuum inside the chamber reached 10^{-9} Torr the crystal was inspected with XPS. Part of the survey spectrum of the crystal without cleaning procedures is displayed in Fig. 4. There is some carbon contamination but the Nb 3p and Nb 3d lines are clearly discernible. We avoided typical cleaning procedures (Ar ion sputtering) and Auger analysis because of surface charging in these insulators.

High resolution spectra for Nb 3d, C 1s and O 1s were obtained before and after exposure to 100 L of CO_2. The high resolution scans for C 1s and O 1s are composed of only one peak for each different chemical state of either C or O. The scan for Nb 3d shows two peaks for each chemical state of Nb. These two peaks correspond to the splitting of the Nb 3d multiplet ($3d_{3/2}$ and $3d_{5/2}$) due to ionization.

The surface of the crystal contains a mixture of Nb^{5+} and Nb^{3+} ions when CO_2 is adsorbed as shown in Fig. 5a (top line). In this scan there are four peaks present due to the Nb 3d multiplet splitting but they correspond to only two different chemical states. When the Nb^{3+} state is removed (Fig. 5a, lower line), the Nb^{5+} state shows two peaks which correspond to its $3d_{5/2}$ (around 206 eV) and $3d_{3/2}$ levels (around 209 eV).

The presence of CO_2 on the surface is detected by a small shoulder on the left side of the O 1s line (top line of Fig. 5c) at a binding energy of 533.2 eV. The C corresponding to CO_2 is not discernible from the C 1s spectrum because the line corresponding to hydrocarbon contamination is too strong (see top line of Fig. 5b).

Since the crystal was provided with electrical contacts on the edges, 2.5 kV was applied on one pair of contacts without removing the crystal from

Table 1
Adsorption volume of N_2 and CO_2 by samples of lithium niobate with different main particle sizes

Main size (μm)	Area (m^2/g)	N_2 counts	N_2 volume (ml)	CO_2 counts	CO_2 volume (ml)	CO_2/N_2
50	0.91	988	0.65	133	0.075	0.115
100	0.42	459	0.30	35	0.020	0.067
200	0.30	328	0.22	–	–	–
500	0.26	282	0.19	–	–	–
1000	0.25	274	0.18	–	–	–
Calibration of 1 ml		1511		1775		

the UHV. XPS inspection after this revealed that most of the CO_2 and the hydrocarbon contamination was removed in this way. After polarizing the crystal with the high voltage only Nb^{5+} was observed on the surface as a clear evidence of structural transfor-

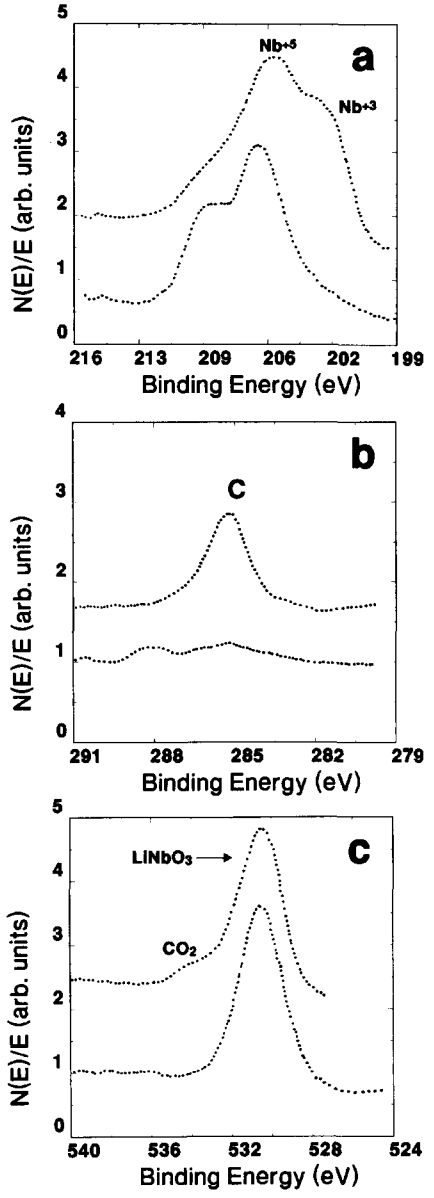

Fig. 5. (a) XPS high resolution scan of Nb 3d lines. (b) XPS high resolution scan of C 1s line and (c) XPS high resolution scan of O 1s line. Top lines correspond to lithium niobate after 100 L CO_2 exposure and bottom lines correspond to lithium niobate after an applied voltage of 2.5 kV.

Table 2
XPS binding energies (eV) for CO_2 adsorbed on lithium niobate

Line	This work		References			
	State 1	State 2	C-cont.	CO_2-ads.	$KNbO_3$	Nb_2O_3
C 1s	285.0	288.0	284.6 [b]	291.8 [a]	–	–
O 1s	529.8	533.2	–	535.1 [a]	–	–
Nd $3d_{5/2}$	202.0	206.0	–	–	206.0 [b]	202.5 [b]

[a] Ref. [8]. [b] Ref. [15].

mation because of the applied voltage. The spectra for Nb, C and O are shown in Figs. 5a, 5b and 5c, bottom lines, respectively. The binding energies determined in these experiments and their respective reference values are summarized in Table 2.

A voltage of 2.5 kV was applied to the crystal because the saturation field is about 3 kV/cm for this material. The saturation electric field rotates the electric domains of the crystal in the direction of the applied field producing a slight change in surface structure.

These results are consistent with Pacchioni's model of CO_2 adsorption on oxides due to surface basicity. Two main conclusions of these experiments are consistent with his model. First, more CO_2 is adsorbed onto small particles of lithium niobate than onto larger particles due to changes in surface morphology. Second, XPS reveals that adsorption of CO_2 and hydrocarbons is related to the presence of Nb^{3+} atoms on the surface.

4. Concluding remarks

We realize that a possible interaction mediated by a dipole–dipole coupling between the CO_2 molecules and the ferroelectric substrate was not the only interaction present in the complex mechanism of CO_2 adsorption by the oxide. Nevertheless, we hoped that this interaction could be competitive in strength with the adsorption interaction arising from charge transfer mechanisms.

The difference relies on more localized interaction at an atomic scale in the case of charge transfer rather than a more macroscopic interaction between the dipole of the CO_2 molecule and the polarization of an electric domain of the crystal.

The results of the XPS experiments suggest that a charge transfer mechanism is mainly responsible for the CO_2 adsorption on this material. In our results, it appears that the local electrostatic potential produced by the configuration of the oxide's surface ions is directly related to the oxide ability for adsorbing CO_2, in agreement with Pacchioni's work on other non-ferroelectric oxides.

Adsorption results on powders of the material show that for large particle sizes (larger than 200 μm), the amount of CO_2 is too small to be detected by our method. One could quickly speculate that the surface of the ferroelectric crystal is still responsible for the adsorption since 32.5% of the surface of barium titanate [1] is covered by CO_2 while only 6.7% of the lithium niobate surface is covered under the same experimental conditions (one must bear in mind that the spontaneous polarization in barium titanate is much larger than in the case of lithium niobate).

Our experimental results are still elusive to prove this point. We are planning future experiments with other ferroelectric materials and even smaller particle sizes in which a ferroelectric behavior is not observed at all.

This effect could have revolutionary technological implications in the areas of gas separation or gas sensors if one can demonstrate that the adsorption of other polar molecules can also be manipulated by a change in the surface structure of ferroelectric materials.

Acknowledgements

This research was partially funded by a grant from the Chilean Government (Fondecyt 1940696). Some of the equipment used in this research was donated by Fundacion Andes.

References

[1] A.L. Cabrera, F. Vargas and R. Zarate, J. Phys. Chem. Solid, 55 (1994) 1303.
[2] R.J.H. Voorhoeve, AIP Conf. Proc. 18 (1974) 19.
[3] H. Suhl, AIP Conf. Proc. 18 (1974) 33.
[4] G. Parravano, J. Chem. Phys. 20 (1952) 342.
[5] T. Kawai, K. Kuninoki, T. Kondow, T. Onisii and K. Tamaru, Z. Physik. Chem. NF 86 (1973) 268.
[6] A.L. Cabrera, B.C. Sales, M.B. Maple, H. Suhl, G.W. Stupian and A.B. Chase, Mater. Res. Bull. 14 (1979) 1155.
[7] A.L. Cabrera, PhD Thesis, University of California, San Diego, La Jolla CA, 1980.
[8] G. Pacchioni, Surf. Sci. 281 (1993) 207.
[9] G. Pacchioni, J.M. Ricart and F. Illas, J. Am. Chem. Soc. 116 (1994) 10152.
[10] J.F. Scott and C.A. Paz de Araujo, Science 246 (1989) 1400.
[11] After S. Brunauer, P.H. Emmett and E. Teller (BET), J. Am. Chem. Soc. 60 (1938) 309.
[12] C.A. Luengo, A.L. Cabrera, H.B. MacKay and M.B. Maple, J. Catal. 47 (1977) 1.
[13] A.L. Cabrera, J. Vac. Sci. Technol. A 7 (1989) 2681.
[14] P.H. Emmett and S. Brunauer, J. Am. Chem. Soc. 59 (1937) 1553.
[15] G.E. Muhlenberg, Handbook of X-Ray Photoelectron Spectroscopy (Perkin-Elmer, Eden Prairie, MN, 1978).